

# Single Grain (U-Th)/He Ages from EET14074, an Acapulcoite Meteorite

**Christian Anderkin**

*College of Liberal Arts and Sciences, University of Florida*

Faculty mentor: Kyle Min, Department of Geological Sciences

## Abstract

EET14074 is a member of the acapulcoite-lodranite family of meteorites and was discovered in Antarctica in 2014 by the Korean Polar Research Institute (KOPRI). Herein, we obtained (U-Th)/He ages from 20 phosphate aggregates in EET14074 to constrain the sample's thermal history. The ages range between  $116.8 \text{ Ma} \pm 145.7 \text{ Ma}$  ( $1\sigma$ ) and  $4211.5 \text{ Ma} \pm 1089.1 \text{ Ma}$ , with an average of  $2530 \pm 260 \text{ Ma}$  ( $n=20$ ). Excluding outlier ages with large uncertainties, the 13 most concentrated ages yielded a theoretical minimum age of  $3000 \pm 150 \text{ Ma}$ . This age corresponds to a fraction helium loss ( $f$ ) of  $\sim 31\%$  assuming crystallization age of  $\sim 4.55 \text{ Ga}$ . The uranium abundances in single aliquots are in the range of 1.52 - 289.93 fmol, with an average of 58.00 fmol ( $n = 20$ ), whereas the thorium abundance ranges between 2.51 and 2337.06 fmol with an average of 1149.29 fmol ( $n = 20$ ). To explain the observed He loss, thermal diffusion modeling was performed with an assumption that the He loss occurred during a recent passage of the meteorite in Earth's atmosphere. For the most likely t-T condition of compressional heating in Earth's atmosphere of this meteorite ( $T = \sim 430 \text{ }^\circ\text{C}$ ,  $t = \sim 10 \text{ sec}$ ), a fractional loss of 29.3% was calculated when the diffusion domain radius ( $r$ ) of  $92.8 \text{ }\mu\text{m}$  was assumed. This estimation is nearly indistinguishable from the observed fractional loss of 31.3%. Additionally, diffusion modeling for another set of data with a different size ( $r = 40.4 \text{ }\mu\text{m}$ ) yielded a very similar fractional loss. Therefore, the observed (U-Th)/He age distribution is likely derived from compressional heating during the passage of EET14074 in Earth's atmosphere.

## Introduction

The decay of naturally-occurring radioactive isotopes has historically proven to be reliable in its providence as a geo-and-thermochronometer (Chang & Qiu, 2012). Additionally, the large variety of radioactive isotopic systems available to the researcher afford solutions to an equally wide range of geologic questions. The (U-Th)/He system is of interest in this context, as it acts particularly well as an effective low-temperature thermochronometer. The cornerstone of (U-Th)/He thermochronometry is based upon the  $\alpha$ -decay of uranium and thorium into lead. These elements are commonly found as minor impurities in phosphate minerals, and their abundances, when compared to the amount of  $^4\text{He}$  atoms present in a geological sample, can be used as an indicator for how long the decay system has been left undisturbed. If the radiogenic  $^4\text{He}$  atoms are left totally undisturbed, the calculated (U-Th)/He age is interpreted as being representative of

the crystallization age. This is often not the case, however, as  $^4\text{He}$ , the lightest noble gas, can very easily diffuse out of the system. This sensitivity is due both to helium's chemical properties (it is an inert gas and, thus, is not incorporated into mineral structures) as well as its small radius, which allows it to easily escape through microscopic fractures in host minerals. For  $^4\text{He}$  to stay within the system, the grain must not be subject to temperatures above the system's designated closure temperature ( $T_c$ ). The established  $T_c$  for the (U-Th)/He system ranges from 55 °C-110 °C (Chang & Qiu, 2012). Diffusion rates are dependent on several variables, the most pertinent of which is temperature as the rate of diffusion of  $^4\text{He}$  out of a mineral system corresponds to increases in temperature. Because of this, the system can be reset by events and processes characterized by high temperatures. Taking this relationship into account, a (U-Th)/He ages can be interpreted as being representative of the time when the dated grain became subject to a temperature at which helium stopped diffusing out, known as its closure temperature. In this case, closure temperature is described by the following equation:

$$T_c = R/[E \ln(AD_0a^2)] \quad (1)$$

Where  $T_c$  in (1) represents the closure temperature,  $R$  represents the gas constant,  $E$  represents the activation energy,  $\tau$  represents the time constant, and  $a$  represents the diffusion domain size,  $A$  represents the value obtained from the established mineral geometry, and  $D_0$  represents the pre-exponential factor (Ehlers & Powell, 1994). The equation for the parent-daughter relationship between uranium, thorium, and helium is as follows:

$$^4\text{He} = 8^{238}\text{U}[\exp(\lambda_{238t})-1]+7^{235}\text{U}[\exp(\lambda_{235t})-1] +6^{232}\text{Th}[\exp(\lambda_{232t})-1] \quad (2)$$

Where  $^{238}\text{U}$ ,  $^{235}\text{U}$ , and  $^{232}\text{Th}$  correspond to the number of parent atoms identified in the sample,  $\lambda$  corresponds to the decay constants for each isotope, and  $t$  is the measured (U-Th)/He age (Chang & Qiu, 2012). Equation (2) numerically describes this relationship. In short, the (U-Th)/He method takes advantage of the accumulation of  $^4\text{He}$  isotopes that are emitted while  $^{238}\text{U}$ ,  $^{235}\text{U}$ , and  $^{232}\text{Th}$  decay into  $^{206}\text{Pb}$ , which become trapped within the crystal lattice of the phosphate grains.  $^{147}\text{Sm}$  also contributes to the gross amount of  $^4\text{He}$  contained within the system via  $\alpha$ -decay (it undergoes one step of  $\alpha$ -decay and emits one  $^4\text{He}$  atom before it reaches its stable daughter particle,  $^{143}\text{Nd}$ ) but its contribution to the gross amount of  $^4\text{He}$  is negligible compared to the contributions of  $^{238}\text{U}$ ,  $^{235}\text{U}$ , and  $^{232}\text{Th}$  (Reiners, 2002). For the samples in this study, the

inclusion of Sm-produced radiogenic helium results in a percent-age difference of less than 0.05. Thus, exclusion of Sm does not result in a meaningfully different age. Low-temperature thermochronology, when applied to meteoritic material, has the ability to provide constraints on the answers to several important questions. Chief amongst them is perhaps the most general question of how asteroidal material has been dispersed and affected by impact events in the post-condensation stage of the solar system (Anders, 1971). The employment of low-temperature thermochronology has also more recently been suggested in the search for instances of interplanetary biomolecule transportation, as impacting events are the primary source of mass transfer between asteroidal and planetary bodies (McKay et al., 1996).

### Sample Descriptions

The sample from which the grains were derived is labeled EET14074. EET14074 is a member of the acapulcoite-lodranite family of meteorites and was discovered in Antarctica in 2014 by the Korean Polar Research Institute (KOPRI). An in-situ photograph is provided in Figure 1. Despite their lack of chondrules, the thermochronologic age of acapulcoites is estimated to be approximately 4.5 Ga ( $4.7 \pm 0.3$  – K-Ar method,  $4.60 \pm 0.03$  – Sm-Nd method,  $4.503 \pm 0.022$  –  $^{39}\text{Ar}$ - $^{40}\text{Ar}$  method) (McCoy et al., 1996) similar to the age of the solar system. Because of these anomalous features, the mineral constitution of acapulcoites has been the subject of a great body of research.



**Figure 1.** A photograph of EET14074 as it was found near Elephant Moraine. This image exhibits the size of the sample as it was found, as well as some of its superficial characteristics. The dark black fusion crust (indicative of atmospheric ablation) is also visible.

The acapulcoite-lodranite family in general is known for its similar mineral chemistry to that of normal, ordinary chondrites (OCs) despite stark differences in their petrologic characteristics. Acapulcoites lack distinct chondrules and show evidence of extensive igneous and metamorphic activity that occurs deep within large asteroids, but are mostly composed of the same major minerals as OCs (olivine, orthopyroxene, plagioclase, phosphates, nickel-iron metal and iron sulfides). In acapulcoites, these minerals have been observed as being arranged in an equigranular texture that is indicative of in-situ recrystallization processes. Additionally, fayalite percentages in olivine tend toward an average of  $Fa_{10.1}$  ( $N = 11$ ; range  $Fa_{9.8-10.4}$ ), indicative of a Mg-rich, forsteritic composition, while low-Ca pyroxenes average at  $Fs_{10.6 \pm 0.4}$  and  $Wo_{1.7 \pm 0.5}$  ( $N = 11$ ; range  $Fs_{10.1-11.4}$ ), which are also indicative of a Mg and enstatite-rich composition (McCoy et al., 1996). Due to their anomalous ages and mineralogy, acapulcoites have also been subject to extensive (U-Th)/He analysis, and are of interest because their namesake, the Acapulco meteorite, has elicited the oldest reliable (U-Th)/He ages reported for any geologic specimen ( $4584 \pm 51$  Ma) (Min et al., 2003). This study is concerned primarily with the phosphate minerals hydroxylapatite, fluorapatite, chlorapatite and merrillite. The major and minor phases present in the sample (including fluorapatite) are visualized in Figure 2.

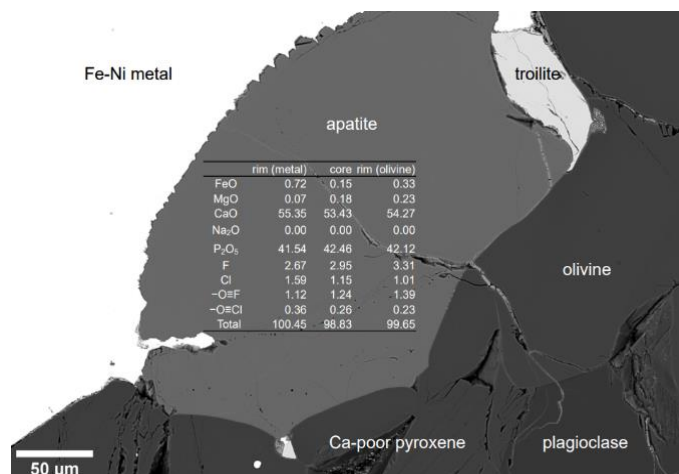


**Figure 2.** SEM image of multiple phases in a thin section, highlighting the oxide mineral content of a Cl and F-deficient apatite phase adjacent to Fe-Ni metal and olivine. Images and oxide data were provided by KOPRI.

## Methods and Procedures

All analyses were performed in-house at the University of Florida Department of Geological Sciences. A small amount (<0.5 g) of the EET14074 rock chip was gently crushed in a ceramic mortar and pestle until it had been granulated. The grains were then placed into a small tube and spread out onto glass slide coated in copper tape and prepared for scanning electron microscopy (SEM). A Zeiss SEM with EDAX Energy-Dispersive X-ray Spectroscopy (EDS) capabilities were employed to identify phosphate-bearing aggregates. Additionally, it was particularly good at holding the grains in place. EDS “field” scans - consisting of several grains - were captured to identify phosphate-bearing aggregates, followed by secondary, more magnified EDS scans of individual phosphate grains. The secondary scans served to identify each grain’s major element chemistry. Phosphate grains with adequate amounts of phosphorus and calcium were selected to be picked to ensure adequate amounts of U and Th, and spatial-chemical mappings of these grains were induced by EDS. A semi-qualitative chemical analysis was performed using EDS to sort identified phosphates into separate mineral classes (chlorapatite, merrillite, hydroxylapatite, and fluorapatite). Grains were removed from the SEM and brought to a Leica petrographic stereoscope. Surface areas of phases were mapped with ImageJ software. Phosphorus-rich (P) surface area was used as a proxy for phosphate surface area because P is homogeneously distributed throughout the crystal lattice of in phosphates.

Using the Leica petrographic microscope and tweezers, the preselected phosphate grains were picked off of the copper tape, placed into 500  $\mu\text{m}$ -wide platinum tubes, and individually put into a concave glass slide, where they remained until  $^4\text{He}$  extraction. After the 20 samples had been put into separate labelled concave glass slides, they were placed into a metal planchette which functioned both as a platform on which grains could be heated, as well as a coordinate system on which the phosphate grains would be organized. The filled planchette was then transferred to the  $^4\text{He}$  analytical system and bolted by hand to the platform.

The current standard procedure for  $^4\text{He}$  extraction consists of placing phosphate aggregates into a high-vacuum environment and heating the samples to a temperature of  $\sim 900\text{-}1250$   $^{\circ}\text{C}$ . To prevent total vaporization of the samples during heating and to avoid any loss of samples, samples were individually placed into platinum tubes. This environment ensures that all of the  $^4\text{He}$  is evacuated from the sample and collected without any helium loss to the environment or helium contamination from the atmosphere (Reiners and Nicolescu, 2006). This was done to

ensure that the degassing process occurred under an ultra-high vacuum ( $1 \times 10^{-9}$  torr). The  $^4\text{He}$  degassing process consisted of 6 sequential stages, and these stages were repeated for every sample. Durango apatite grains were also measured as a standard. After the  $^4\text{He}$  was measured, the planchette and grains were removed from the degassing system and transferred to labelled Teflon vials where they were introduced to 50 ml of a spiked solution containing  $7.55 \pm 0.10$  ng/ml  $^{233}\text{U}$ ,  $12.3 \pm 0.10$  ng/ml  $^{229}\text{Th}$ , and  $10.8 \pm 0.10$  ng/ml  $^{147}\text{Sm}$ . Apatite grains were then dissolved for 1 hour at 90 C in 5% nitric acid. The solutions were then analyzed for U, Th and Sm isotopic ratios by inductively-coupled plasma mass spectrometry (Nu Plasma ICP-MS) (Reiners and Nicolescu, 2006). Calculations were made with Microsoft Excel.

### Results

Given that the thermochronologic age of acapulcoites is estimated to be approximately 4.5 Ga ( $4.7 \pm 0.3$  – K-Ar method,  $4.60 \pm 0.03$  – Sm-Nd method,  $4.503 \pm 0.022$  –  $^{39}\text{Ar}$ - $^{40}\text{Ar}$  method) (McCoy et al., 1996) and the meteorite examined was designated as unshocked, deviation from this age is interpreted as being indicative of thermal heating events. The calculated ages range between 116.8 Ma  $\pm$  145.7 Ma (uncertainties are reported at  $1\sigma$ ) and 4211.5 Ma  $\pm$  1089.1 Ma ( $n = 20$ ) with an average age of  $2530 \pm 260$  Ma (Figure 5). Possible explanations for this relative deviation from the established age include possible thermal events, possible incorporation of helium into apatite from cosmic ray exposure, and helium diffusional kinetics (Ehlers & Powell, 1994). The ejection of  $^4\text{He}$  nuclei from the outer 20  $\mu\text{m}$  of a grain can also result in anomalously young (U-Th)/He ages, especially when considering mineral grains that have higher surface area to volume ratios (Min et al., 2003).

Thus, it is believed that larger apatite grains will yield smaller analytical errors, as the signal-to-noise ratio is higher in grains with greater amounts of U and Th (Min et al., 2003). This assumption was generally supported by our data, as larger grains exhibited smaller errors (Figure 3). Here, the elicited (U-Th)/He ages are assumed as being minimum ages. Implicit in this assumption is the expectation of homogeneously distributed uranium and thorium atoms within each aliquot. Figure 4 further elucidates the relationship between grain size and age, relating U+Th+Sm content to age.

Single-aliquot uranium abundances ranged between 1.5 and 290 fmol with an average of 58.0 fmol ( $n = 20$ ), while thorium concentrations ranged between 2.5 and 2337 fmol with an

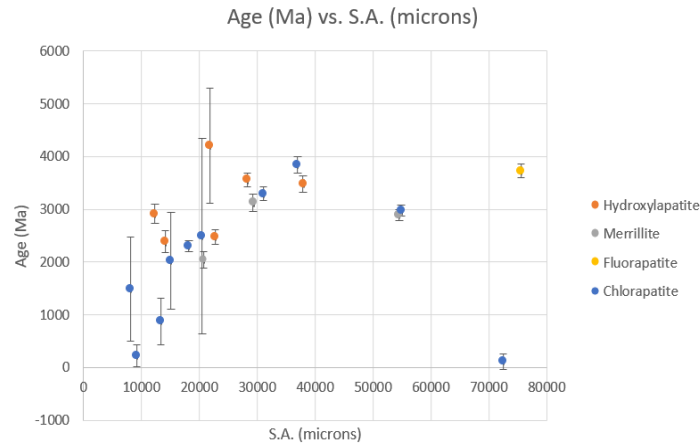


**Figure 3.** The relationship illustrated here supports the hypothesis that there is a correlative relationship between the size of a grain and its apparent age, as well as between its size and standard of error. Here, smaller grains exhibit generally lower ages with greater degrees of uncertainty, while larger grains exhibit both older and more certain ages.

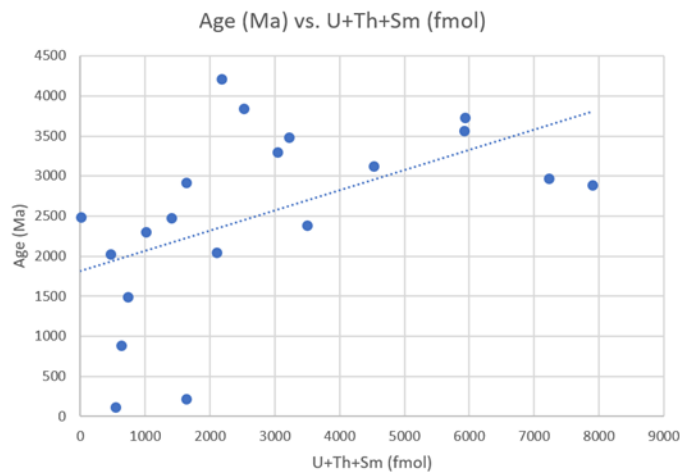


**Figure 4.** Grains with lower abundances of U+Th+Sm exhibit similar behavior to those grains with low surface areas, while grains with higher concentrations of U+Th+Sm exhibit older and less scattered ages.

average of 1149 fmol ( $n = 20$ ). Smaller samples yielded more scattered ages with high degrees of uncertainty, while larger grains generally elicited older and concentrated ages with lower degrees of uncertainty. All measured (U-Th)/He ages yielded an arithmetic mean of  $2530 \pm 260$  Ma (Figure 5). The 13 oldest samples yielded ages more tightly clustered around 3000 Ma (Figure 6) than the data points from all measured ages (Figure 5). The calculated age here corresponds to a theoretical fractional  $^4\text{He}$  loss of 31.3%. We believe that this distribution better represents the apparent (U-Th)/He age of EET14074 and performed thermal modeling for this age data.

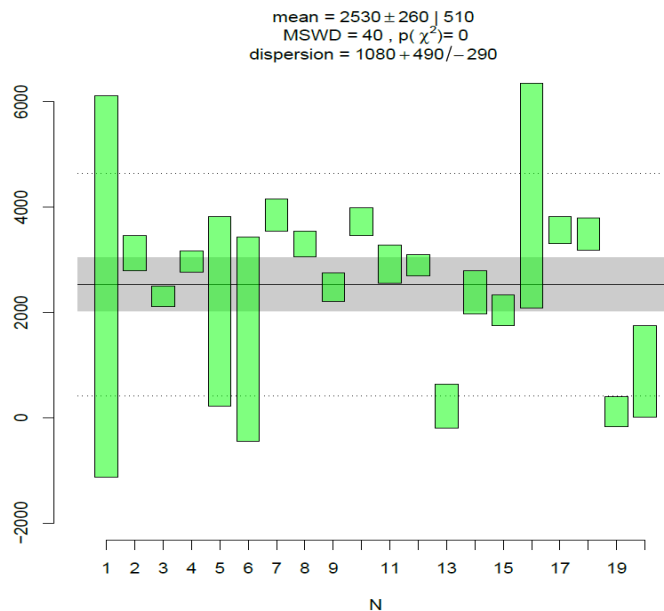


**Figure 5.** The calculated mean age for the sampled grains is tightly clustered around  $2530 \pm 260$  Ma. This dataset includes calculated ages from all aliquots. This represents a total He loss of 44%.

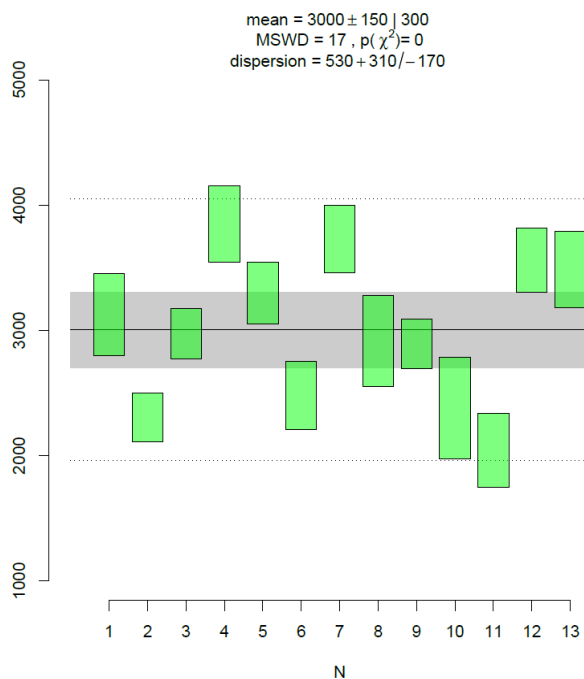


**Figure 6.** The calculated mean age for the 13 oldest sampled grains with high degrees of certainty is tightly clustered around  $3000 \pm 150$  Ma. When the data points with high uncertainties are eliminated, this is the resultant age.



## Discussion

### Morphological Constraints and Thermal Ages

It was observed through the course of this experiment that grains with greater abundances of U+Th+Sm generally yielded older ages (Figure 4). Despite this relative similarity, the 13 oldest grains (Figure 6) exhibited spuriously young ages compared to the weighted mean of the five oldest ages described by (Min et al., 2003)  $4538 \pm 823$  Ma). In order to explore the hypothesis that grain size and morphology might have an effect on the reliability of ages, we mapped surface areas of phases that were designated as phosphorus-rich. An example of one such area is provided in Figure 7. The data we gathered suggests that there is a correlative relationship between calculated P-rich surface area and calculated U+Th+Sm content. This relationship is illustrated in Figure 8. One possible explanation for the deviation of these grains from the accepted age is the result of grain morphology and differences in the parameters describing the kinetic behavior of helium within apatite grains.

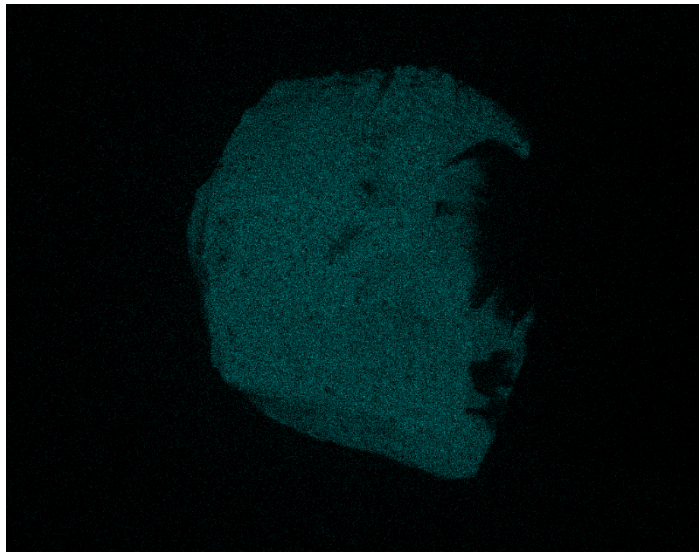


**Figure 7.** An SEM image of a phosphorus-rich phase induced by EDAX energy-dispersive X-ray spectroscopy (EDS). Blue areas indicate phosphorus-rich zones. The scale for this image is 0.286 microns per pixel.

### Thermally-induced He Loss

A primary assumption underlying this experiment was that the meteorites we studied are unshocked. This assumption is justified by thin-section examinations made by KOPRI (Figure 2). Thus, the most likely thermal event to induce helium loss within our sample is related to

compressional heating that is experienced by the meteorite during its passage through the atmosphere. To constrain proposed atmospheric time-temperature paths, diffusion-modeling was employed using established kinetic parameters (Ehlers & Powell, 1994). To eliminate theoretical uncertainty regarding phosphate depth (z-axis) morphological constraints, a spherical geometry was assumed with a radius of 92.79  $\mu\text{m}$ . The radius was calculated using the collected surface area data, which acts as a proxy for size. For diffusion modeling, we assumed that a single isothermal heating event caused the observed helium loss. The most likely temperature conditions ( $T = 430^\circ\text{C}$ ) over a designated period of time ( $t = 10$  seconds) are combined with the observed mean diffusion domain radius (92.79  $\mu\text{m}$ ). The simulated variables here are used to simulate a compressional heating event upon collision with the Earth's atmosphere. The simulated diffusion parameters for chlorapatite as referenced in Min et. Al. (Min et al., 2003) were as follows:  $E_a = 44.2$  kcal/mol, and  $D_o = 4.2 \times 10^6$   $\text{cm}^2/\text{sec}$ . The accuracy of this geometry was tested in Figure 9. The diffusional kinetics of helium were modeled at the previously listed values ( $T = 430$  C,  $t = 10$  seconds,  $r = 92.79$   $\mu\text{m}$ ,  $E_a = 44.2$  kcal/mol, and  $D_o = 4.2 \times 10^6$   $\text{cm}^2/\text{sec}$ ), and a fractional loss of 29.3% was calculated.

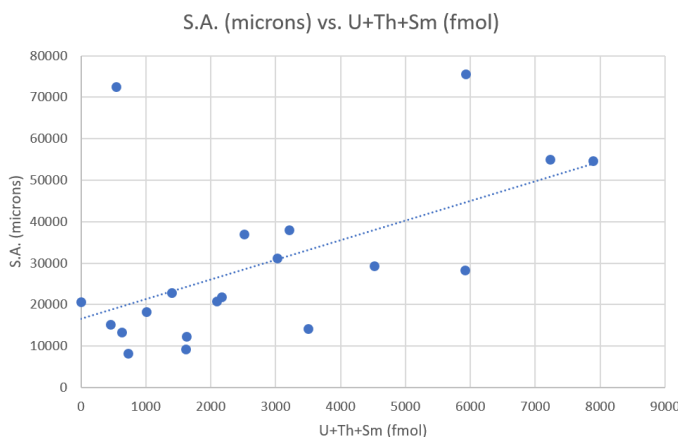


**Figure 8.** This positively correlated relationship supports the assumption that U+Th+Sm content can be used as a viable proxy for grain size (and vice versa).

### Alpha-Recoil Correction

The method applied by Farley et. al. (1996) was used to relate alpha-recoil correction to our set of sampled grains. The implication herein is that for a grain to lose a specified amount of He, the diffusion domain must have a corresponding diffusion domain size and must be subject to a specific temperature. Alpha recoil correction attempts to correct for the amount of

helium that is lost, so that the corrected age better represents the ‘pristine’ age. The  $r$  value used for diffusional modeling ( $r = 92.79 \mu\text{m}$ ) was retained in the Analytical Model (Figure 10) (Farley et. al. 1996) used to quantify alpha-retentivity. The model derived from (Farley et. al. 1996) relating alpha-retentivity ( $F_T$ ) and radius ( $r$ ) is displayed in Figure 10.

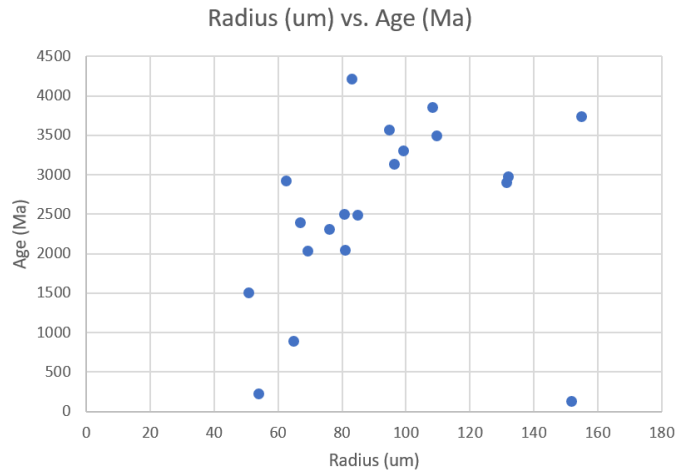


**Figure 9.** The trend depicted here is a positive relationship between S.A. and age. This relationship supports the assumption that a spherical geometry is accurate and can, in this case, be used for thermochronologic analysis.

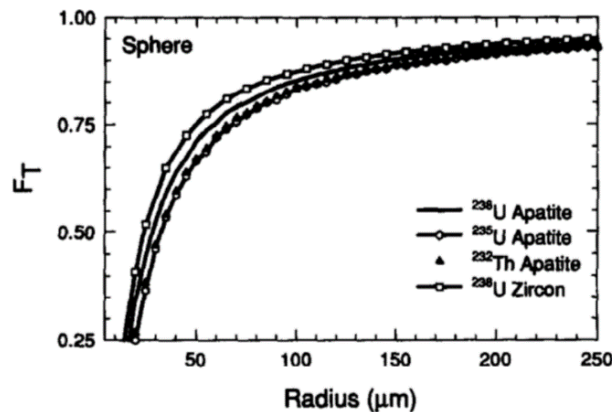


**Figure 10.** The model derived by (Farley et. al. 1996) relates the variables  $r$  and  $F_T$ , indicating a clear relationship between the approximate mean radius of a granular data set and the data set’s alpha-retentivity. Graph provided with reference to Farley et al.

## Conclusion

Thermochronologic studies of meteorites and asteroidal material can be used to provide constraints and context for the metamorphic and thermal histories of asteroidal bodies throughout the solar system, as well as for delivery of their materials to the Earth's surface. Granular uranium abundances ranged between 1.52 and 289.93 fmol, with a mean abundance of 58.03 fmol ( $n = 20$ ), while thorium abundances ranged between 2.51 and 2337.06 fmol with a mean of 1149.29 fmol ( $n = 20$ ). Smaller samples exhibited a general trend of scattered ages with high degrees of uncertainty, while larger grains generally elicited older ages with lower degrees of uncertainty. The calculated ages exhibited a relatively high degree of uncertainty and ranged between  $116.8 \text{ Ma} \pm 145.7 \text{ Ma}$  (uncertainties are reported at  $1\sigma$ ) and  $4211.5 \text{ Ma} \pm 1089.1 \text{ Ma}$  ( $N = 20$ ) with an average age of  $2530 \pm 260 \text{ Ma}$  (Figure 5). 13 of the oldest sampled grains are tightly clustered around  $3000 \pm 150 \text{ Ma}$  and exhibit a distribution with a lesser degree of variance than the data points depicted in the raw data set, and thus, is representative of the apparent age. In this study, we determined that the probable explanation for phosphate ages that exhibit deviance from the "undisturbed" age of  $\sim 4583 \text{ Ma}$  can be explained by an isothermal heating event defined by the parameters  $T = 430 \text{ C}$ ,  $t = 10 \text{ seconds}$ ,  $r = 92.79 \text{ }\mu\text{m}$ ,  $E_a = 44.2 \text{ kcal/mol}$ , and  $D_o = 4.2 \times 10^6 \text{ cm}^2/\text{sec}$ . The modeled fractional  $^4\text{He}$  loss was found to be 31.3%, which was very close to the observed fractional loss value (29.3%), granting an initial degree of confidence to this time-temperature path. Another independent diffusion modeling performed for a different diffusion domain size (Sheikh, 2018) yielded essentially identical t-T conditions. This finding allows us to place a much greater degree of confidence in this proposed time-temperature path.

## References

- Anders E. (1971). Meteorites and the early solar system. *Annual Reviews in Astrophysics and Astronomy* 9, 1-34.
- Chang, J., & Qiu, N. (2012). Closure temperature of (U-Th)/He system in apatite obtained from natural drillhole samples in the Tarim basin and its geological significance. *Chinese Science Bulletin* 57, 3482-3490.
- Ehlers K & Powell R. (1994). An empirical modification of Dodson's equation for closure temperature in binary systems. *Geochimica et Cosmochimica Acta* 58, 241-248.

- Farley, K., Wolf, R., & Silver, L. (1996). The effects of long alpha-stopping distances on (U-Th)/He ages. *Geochimica Et Cosmochimica Acta* 60, 4223-4229. doi:10.1016/s0016-7037(96)00193-7
- McCoy, T.J., Keil, K., Clayton, R.N., Mayeda, T.K., Bogard, D.D., Garrison, D.H., Huss, G.R., Hutcheon, I.D., Wieler, R. (1996). A petrologic, chemical, and isotopic study of Monument Draw and comparison with other acapulcoites: Evidence for formation by incipient partial melting, *Geochimica Cosmochimica Acta* 60, 2681-2708.
- McKay, D.S., Gibson Jr. E.K., Thomas-Keprta, K.L., Vali, H., Romanek, C.S., Clemett, S.J.,... Zare, R.N. (1996). Search for past life on Mars: Possible relic biogenic activity in Martian meteorite ALH84001, *Science* 273, 924-930.
- Min, K., Farley, K., Renne, P., Marti, K. (2003). "Single grain (U-Th)/He ages from phosphates in Acapulco meteorite and implications for thermal history." *Earth and Planetary Science Letters* 209, 323-336.
- Reiners, P. W. (2002). (U-Th)/He chronometry experiences a renaissance, *Eos*, 83(3), 21-27,
- Reiners, P.W. & Nicolescu, S. (2006). Measurement of parent nuclides for (U-Th)/He chronometry by solution sector ICP-MS, *ARHDL Report 1*, <http://www.geo.arizona.edu/~reiners/arhdl/arhdl.htm>
- Sheikh, D. (2018). Personal Communication